

---

# The Tunneling Microscope: A New Look at the Atomic World

J. A. GOLOVCHENKO

---

**A new instrument called the tunneling microscope has recently been developed that is capable of generating real-space images of surfaces showing atomic structure. These images offer a new view of matter on an atomic scale. The current capabilities and limitations and the physics involved in the technique are discussed along with specific results from a study of silicon crystal surfaces.**

---

**T**HE POSSIBILITY OF SEEING ATOMS FASCINATES SCIENTISTS and nonscientists alike. Researchers around the world are currently building a new kind of instrument called the tunneling microscope (1), which, pushed to its ultimate capability, appears to provide real-space pictures of atomic structure. In this article I shall discuss how the instrument works, its accomplishments to date, its inherent strengths and limitations, and what we may expect from it in the future.

It is essential to realize at the onset that the drive to understand the microscopic structure of matter has had profound consequences for us all. From the shapes of the simplest molecules in our atmosphere to the arrangement of atoms in crystals and the macromolecules of life, understanding of structure has led to understanding of function, which in turn has led to synthesis and even controlled modification of our environment. Historically, the main tools that have been brought to bear on the problem of elucidating atomic structure have made use of the diffraction of waves. Here a finely collimated beam of x-rays, electrons, or perhaps neutrons collides with and is scattered by the atomic system under study. Analysis of the angular pattern formed by the scattered beam gives information about the arrangement of atoms in the system. Yet, most would agree that in diffraction experiments individual atoms are not seen. One requires many atoms (either in the form of many small molecules or one very large one, such as a crystal) to obtain the desired structural information, which comes out as an average property of the large system.

There are means by which one does get the sense of seeing atoms, and it is to this class of methods that tunneling microscopy belongs. The first images of atoms were obtained with the field ion microscope (2). In this instrument, invented by Erwin Müller, the sample is a fine needle, usually a metal like tungsten, which is placed in front of a fluorescent screen in a chamber containing a minute amount of helium. When a high positive voltage is applied to the needle, helium atoms at certain atomic sites are ionized by field-induced electron tunneling from the helium atoms into the needle. The same

applied field then accelerates the resulting helium ions into the fluorescent screen, where a greatly magnified image of the individual atomic sites near the end of the needle is formed. A second method by which images of atoms can be obtained is with the electron microscope (3). The principle of operation is similar to that of a typical optical microscope, except that light waves are replaced by short wavelength electrons and glass lenses by electromagnetic ones. It has been shown by Crewe *et al.* that heavy atoms in a lighter matrix can be imaged under favorable circumstances (4). Recent progress on the imaging of atomic planes near crystal surfaces has also been reported (5). The newest development in this area is the tunneling microscope, developed a few years ago by Binnig *et al.* (1). The physical principles on which this device operates are similar to those of the field ion microscope, but it has several fundamental advantages in execution that promise to make it far more useful.

## Principles of Operation

Tunneling is a common phenomenon on the atomic scale wherein nature permits electrons to penetrate (tunnel) into classically forbidden regions of space where the particle potential energy exceeds its total energy. The quantum nature of an electron gives it wavelike properties, and the necessary negative kinetic energy in the forbidden region is a property of damped or evanescent waves. For example, at a sufficiently great distance from the nucleus of an atom, such a forbidden region exists for all bound electrons. The waves representing the electrons here are damped exponentially with increasing distance from the nucleus. The chance of finding an electron at increasing distances decreases correspondingly.

Imagine now that such an atom is at the end of an atomically sharp metallic needle. If we bring this needle close to the surface of a conducting material and put a small potential difference between the two, an electrical current will flow. For gap distances of 5 Å, an applied bias of several tens of millivolts will induce nanoampere current flows. Electrons can flow across the forbidden gap because of the tunneling effect. The current is a strong exponential function of gap spacing, reflecting the exponentially damped nature of the electron wave function there. (It typically declines by one order of magnitude for every angstrom of increase in gap spacing.) If the needle is now scanned across the surface laterally while its distance from the surface is adjusted to keep a constant tunnel current, a topograph of the surface is obtained in the recorded trajectory of the tip.

This method of obtaining a surface topograph was first demonstrated by Young *et al.* (6), who used piezoelectric ceramic elements to raster scan the lateral motion and a feedback control system to keep the gap current constant. However, they were unable to obtain a lateral resolution better than several thousand angstroms. The

---

J. A. Golovchenko is a member of the technical staff, AT&T Bell Laboratories, Murray Hill, NJ 07974.

major step responsible for all the present activity in the field was taken by G. Binnig and H. Rohrer, who improved the vibration isolation, prepared atomically clean surfaces in an ultrahigh vacuum (UHV) environment, used very small gap spacings, and developed methods of gently bringing the tip up to the surface. Their reward was topographs of surfaces that showed atomic structure. At first, atomic steps on apparently flat metal surfaces were observed (7); later, details of atomic reconstructions on metal (8) and semiconductor surfaces (1) were obtained.

## The Instrument

Figure 1 shows a schematic illustration of the main features of such a microscope. A tripod made of piezoelectric ceramic serves as the main manipulator of the tunneling probe tip made of tungsten. Electric fields applied to the ceramic legs through evaporated metallic contacts induce strain in the structure, which moves the tip around. For the instrument constructed at Bell Laboratories, the tripod provides a maximum continuous tip range of 10,000 Å in all directions, with displacement control better than 0.1 Å. The tip motion parallel to the surface to be studied is raster scanned at speeds up to 100 Å/sec by applying triangular voltage waveforms to the  $x$  and  $y$  tripod legs. Square pictures 100 Å on a side therefore can be acquired in a few minutes.

The tip motion perpendicular to the sample surface is adjusted by an integrating feedback system that maintains a constant gap current as the tip is rastered laterally. A voltage source,  $V_{\text{bias}}$ , induces the tunnel current, which is monitored and compared with a reference value, the demanded tunnel current, and a voltage error signal is generated. This voltage is applied to the  $z$  tripod leg to adjust the tip position so that the tunnel current agrees with the reference, which

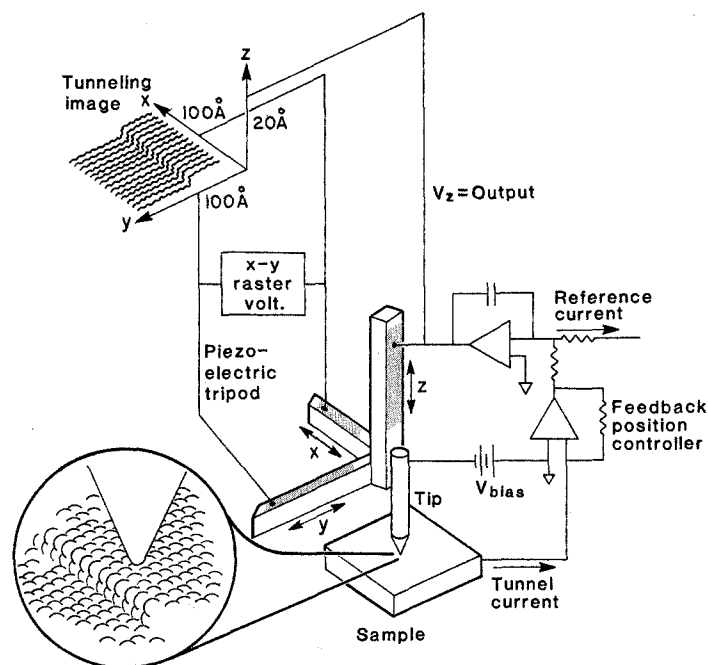


Fig. 1. Schematic illustration of the tunneling microscope. The tunnel current from tip to sample, induced by  $V_{\text{bias}}$ , is maintained constant by an electronic feedback system (right), which controls the tip position normal to the sample surface via the  $z$  leg of the piezoelectric tripod. A record of the  $z$ -leg feedback voltage, as the  $x$ - $y$  tripod legs raster scan the tip laterally, constitutes a tunneling image, which is a kind of replica of the sample surface (inset at bottom). The sample, tip, and tripod are maintained in a vacuum chamber.

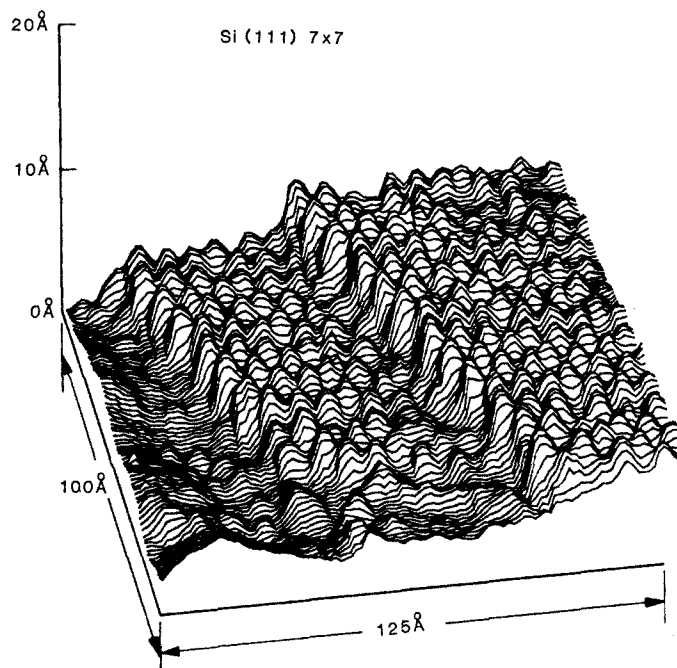


Fig. 2. Tunneling image of silicon (111) surface that shows the  $7 \times 7$  atomic reconstruction on terraces separated by atomic steps.

makes the tip "float" approximately 5 Å above the feature directly below it on the surface. If the calibration of the tripod piezoelectric legs in volts per angstrom is known, then a plot of the feedback-controlled  $z$  piezo voltage as a function of the  $x$  and  $y$  piezo voltages is a kind of tunneling replica of the sample surface, which we generally refer to as a tunneling image.

There are many other experimental details involved in obtaining tunneling images from the microscope. Some of these represent serious problems to experimentalists trying to interpret results produced by their instruments. For example, how does one prepare a tip capable of atomic resolution, bring it to within striking distance of the surface without "crashing," minimize the effects of vibration and thermal drift, and effectively prepare samples of interest for study? The most fundamental problem is to translate the tunneling images into pictures that reflect the identity and position of individual atoms of an unsolved structure. Solutions to the above tend to be part science and part art, and are the subject of continuous discussion and rapid development.

## Applications

The first and main applications of tunneling microscopy have been in the area of surface physics. Crystal surfaces are the seat of many interesting phenomena, both of a practical and fundamental nature. Almost invariably, understanding these requires a detailed knowledge of the atomic structure of the surface. Diffraction methods have been used to probe crystal surfaces and have shown that, in many cases, the surface adopts a structure different from a simple termination of the bulk. The most widely used diffraction method relies on the shallow probing depth of low-energy electrons. Such studies of many surfaces indicate a variety of superlattice structures that the outermost layers adopt to minimize their free energy. This "deviant" outer layer may differ from the bulk crystal by simply being strained or by adopting a completely rearranged bonding configuration several layers deep. Some are so complicated

or subtle that the diffraction methods have failed to completely determine the structure.

A famous example is the silicon (111) surface. Electron diffraction indicates that a superlattice exists in the plane of the surface with a unit cell that is seven times larger laterally in each direction than a simply terminated surface would be. The problem of this so-called silicon (111)  $7\times 7$  surface structure has remained unsolved for 25 years in spite of many hints from a plethora of surface techniques. Tunneling microscopy has provided new insights to this surface and brought us very close to its resolution. Figure 2 shows a tunneling image of a 100 by 125 Å region of silicon (111)  $7\times 7$  obtained at Bell Laboratories. To obtain and maintain surfaces like these, the experiments must be performed in UHV chambers (pressure,  $\approx 1 \times 10^{-10}$  torr). Oxide and hydrocarbon contamination are removed by argon ion sputtering, and the surface is brought to its final state of crystallinity by high-temperature annealing. An electron diffraction apparatus verifies the presence of the reconstructed surface of interest before the tunneling image is obtained.

The scanned tip trajectory from the tunneling microscope is shown in Fig. 2. It indicates several modulated terraces separated by 3-Å vertical atomic steps. The modulation in the terrace regions is roughly 1 Å high. Pictures such as these are the kind our microscope immediately produces in a computer display near the experiment. It can be highly instructive to convert this into a gray-scale picture (Fig. 3). White areas correspond to the high regions in Fig. 2 and dark areas to the low ones. While this view of the surface is not as quantitatively informative about the actual height variations of the tip, it is vastly superior to the line scans for displaying atomic structure and surface symmetry. Outlined in the figure is the  $7\times 7$  rhombic unit cell, originally observed by Binnig *et al.* (1), which is 26 Å on a side. Within the cell are 12 distinct protrusions and, at each corner, a deep depression. It is tempting and probably correct to interpret each of these protrusions as individual silicon atoms that constitute the outermost layer of the crystal. It must be recognized that this layer has only 12 atoms per  $7\times 7$  unit cell compared to a possible 49. This is a favorable case for the tunneling microscope since the tip modulation can be large because of the large distance between these topmost atoms. On viewing images like those in Figs. 2 and 3, the technically inclined are prone to ask what the resolution of the instrument actually is. The empirical answer is that under "favorable" circumstances "features" 2 to 3 Å in lateral extent can be "resolved." The need for quotation marks here will become clear as we proceed.

Figure 2 yields additional information about the particular silicon surface under discussion and suggests other useful capabilities of the microscope for surface physics studies. Atomic steps, clearly visible in Figs. 2 and 3, are in a sense the most fundamental defect on crystal surfaces. Atomic steps can be detected on crystal surfaces in diffraction experiments when they are present at high density in a periodic array (9). Individual steps have been imaged in electron microscopes by replica (10) and interference (11) methods, but none of these methods has yielded the atomic structural detail of the steps as demonstrated here. Knowledge of this type is necessary if we are to understand how crystals grow. For example, when silicon crystals are grown by molecular beam epitaxy, new atoms are continually evaporated onto the surface from some kind of oven. These atoms diffuse across the flat terraces on the surface and are incorporated into the crystal lattice at the atomic steps. The essential chemical reactivity, surface reconstruction, crystal defect concentration, and susceptibility to impurity incorporation may all be dominated by the microscopic processes occurring at the steps. Just as a surface can be reconstructed, so can a step, and such reconstructions may be expected to affect all of the above. The large holes that normally terminate the ( $7\times 7$ ) unit cell corners are incorporated into the

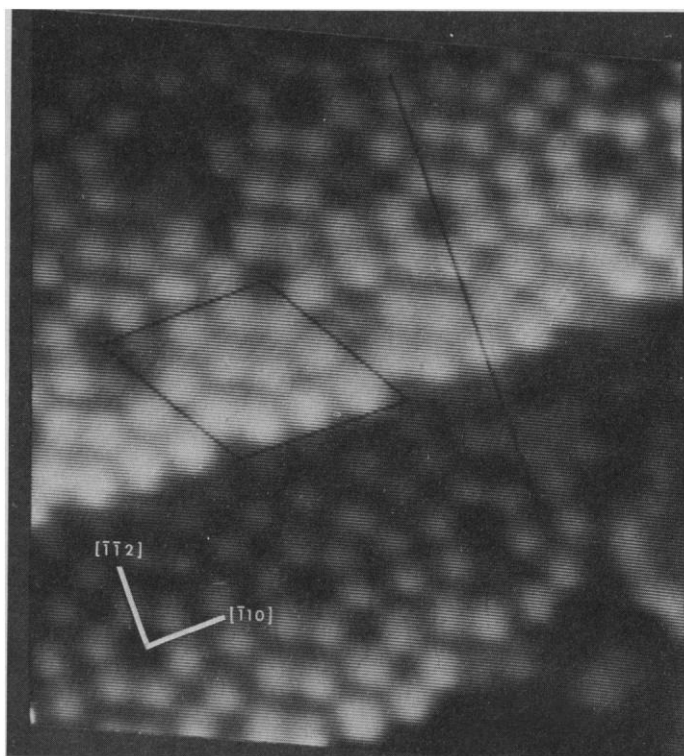


Fig. 3. Gray scale rendering of the tunneling image in Fig. 2. White regions are elevated and dark ones depressed. The rhombic  $7\times 7$  unit cell is indicated, as is the orientation of the surface.

atomic step wall on both the top and bottom sides of the step. There is even a small lateral displacement along the step edge that yields a phase slip between the reconstructions on the top and bottom sides of the step. Details such as these have helped us to form an atomic model for the structure of the  $\langle 112 \rangle$  steps on silicon surfaces. This model has in turn shed light on the nature of the subsurface reconstruction, which is not normally accessible to the tunneling microscope on totally flat surfaces.

## Sample Preparation

There is currently no way to identify the kinds of atoms the microscope is imaging. This is a severe problem because only atomic structure at a surface can be probed and surfaces are prone to contamination from the environment. The most common problems are oxidation and adsorption of water and hydrocarbons. Surfaces can also be contaminated by impurities that migrate there from the underlying bulk. The study of surfaces has become an exact science in recent years only because methods to prepare and maintain atomically clean samples have been developed. These methods are often tedious, time-consuming, and expensive, but without them any results obtained on atomic structure are suspect.

Even these methods (for example, UHV environments, sputter cleaning, high-temperature annealing, low-energy electron diffraction, Auger electron spectroscopy, and so forth) are not the last word on preparing standard equilibrium surfaces for study. Virtually all standard surface characterization techniques average over macroscopic areas of the sample, and in doing so may mask or misinterpret the inhomogeneous character of many surfaces. Here the view provided by the tunneling microscope can yield not only new insights into the structure (12) of the microscopic surface components but also further criteria for evaluating surface prepara-

tion methods. The reader may have noticed surface point defects in Figs. 2 and 3. These are probably due to the incorporation of impurities like carbon during the preparation. There appears to be no other method capable of detecting defects in such low concentrations at the surface. On the other hand, any given view with the tunneling microscope may be the exception rather than the rule in that it corresponds to only a small fraction of the surface area. It can take a long time (and great patience) to obtain enough tunneling images to characterize all the possible topographies that may be present on a surface. (One may often spend several weeks studying a single sample.) Combination of macroscopic probes with the tunneling images is also essential if these results are to be integrated into the field of surface physics in a reliable way.

## The Tip

Having dealt with questions of sample preparation, we come to the crucial question of the tip. The ideal situation, and one that we believe is realized when the microscope operates well, has the tip terminating in a single atom. Currently this situation is obtained only by luck and the fact that the state of the tip is changeable. Atoms may be transferred inadvertently to the tip from the sample or simply diffused there from the tip shank. We have observed the apparent structure of a surface change due to changes in the detailed termination of the tip. Again, it is only patience and intuition gained through experience and familiarity with the system under study that gives confidence that the correct tunneling images are obtained. Progress in this area will probably come from field-ion microscope studies of the tunneling microscope tip itself.

With these caveats, a wide range of topographical studies can be anticipated. The family of semiconductor surfaces is responsible for many unsolved problems in surface physics, and already a number of tunneling images of silicon (13), germanium (12), and gallium arsenide (14) surfaces have been obtained. Metal surfaces were

among the first looked at by Binnig, Rohrer, and co-workers, and charge density wave observations on transition metal dichalcogenides were recently reported by Coleman *et al.* (15). Of course, the tunneling probe requires that conducting or semiconducting materials be used as the base material, but the field of interesting systems is limitless, ranging from elemental surfaces to compounds and alloys to chemically treated surfaces. The idea of using the crystal as a "table" on which to place interesting molecules for study is especially appealing.

Preliminary steps along these lines have already been taken. These range from the study of adsorbed surface atoms through exciting attempts to image large molecules like DNA and even viruses (16). While such studies have yet to provide any essential new insight into macromolecular chemistry or molecular biology, we may hope that our understanding of the physical processes involved in the operation of the microscope with various surfaces and specimens will lead to new views of this domain of our experience.

## Electrical Properties

As already mentioned, a fundamental problem with the tunneling microscope is identifying different kinds of atoms in chemically heterogeneous surfaces. Even after cleaning, the problem arises in surface studies of compounds and alloys as well as in studies of adsorption of foreign atoms on solid surfaces. It is this quest that will most likely drive the quantitative study of the detailed electrical behavior of the probe tip-sample tunnel junction. The hope here is to find some electrical signature that will identify what kind of atom lies below the probe tip. The electrical properties of the junction can be rich indeed, even for an atomically homogeneous system.

The most straightforward junction measurement to obtain from the tunneling microscope is a plot of tip distance versus applied bias for constant tunnel current. Such data are particularly simple to obtain because the feedback system is active and the instrument

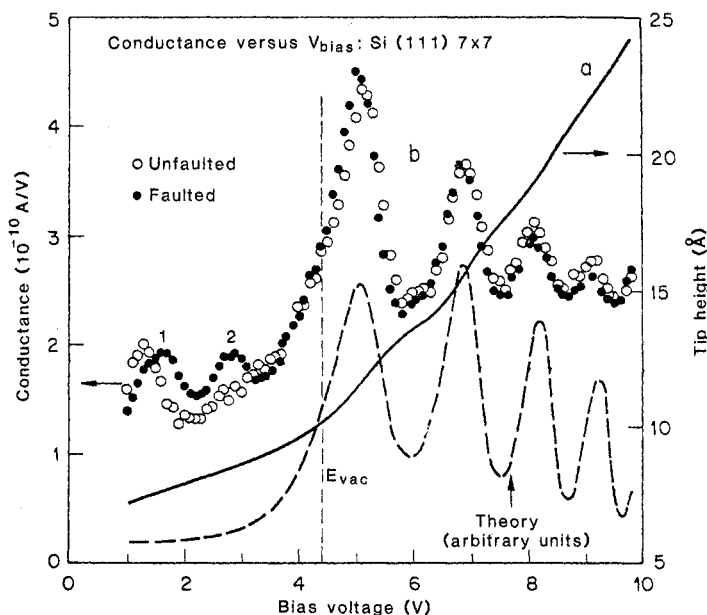
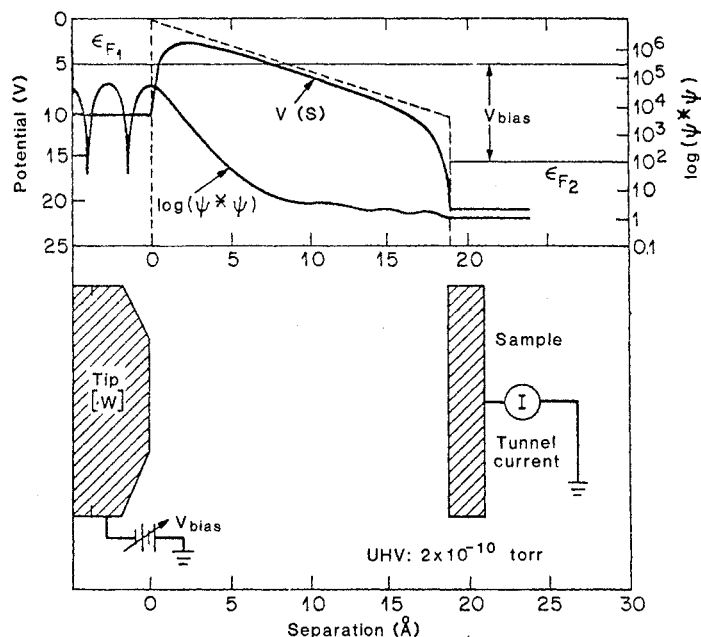


Fig. 4 (left). Mechanical and electrical properties of the tip-vacuum-sample tunnel junction for a silicon (111)  $7 \times 7$  surface. Curve a shows the tip height above the surface versus bias voltage for a tunnel current of 1 nA. Curves b1 and b2 show the electrical conductance of the junction ( $dI/dV_{\text{bias}}$ ) versus bias voltage. The dashed curve shows the theoretical behavior expected from an electron Fabry-Perot interferometer.  $E_{\text{vac}}$  is the deduced vacuum energy level



outside the sample and corresponds to the local work function. Fig. 5 (right). Energy level diagram of tunnel junction used to generate theory curve in Fig. 4. The potential energy curve without (dashed) and with (solid) image potential effects is shown along with the probability density for an electron at the Fermi level. Tunneling occurs only where  $V > \epsilon_{F1}$  on the tip side of the vacuum gap.

operates in a stable way. As the applied gap voltage is increased, the tip must withdraw from the surface to keep a constant tunnel current.

Curve a in Fig. 4 shows the result of this exercise. This kind of curve was first obtained by Young *et al.* (17) in their early microscope studies, in which it was used to identify the different tunneling processes that become operative. Binnig and Rohrer (18) obtained much more detailed curves with their improved instrument that showed additional structure. That structure which is evident in curve a is much enhanced by directly measuring the conductance, which is plotted as curve b in Fig. 4. There are two different regions of interest to us here, which are roughly above and below 4 V of bias.

Above 4 V a regular oscillatory behavior is observed that is explained (19) with the help of the energy level diagram in Fig. 5. For a high applied bias, the tunneling region is restricted to the vicinity of the tip. As the tunneling electron approaches the sample surface, its kinetic energy becomes positive and the wave function describing the electron takes on an oscillatory behavior. When the electron reaches the sample surface, another phenomenon occurs that, like tunneling, can be understood only with the aid of quantum mechanics. At the surface there is a rapid increase in the forces attracting the electron to the body of the solid target. (These are the same forces that are responsible for keeping the valence electrons of the solid from leaving through its surface.) In spite of the fact that the forces are directed into the surface, the rapid variation results in a probability amplitude that the electron will be reflected back toward the tip. Before reaching the tip, the electron is deflected back toward the sample surface by the applied external field, where again part is reflected and part transmitted, and so on. The interference resulting from the addition of all these amplitude components results in the wave function having a partial standing wave character in the gap and an oscillatory behavior in the transmitted current as a function of applied bias and gap spacing. For those familiar with optics we have essentially a Fabry-Perot interferometer for electrons here.

By determining the applied bias where the oscillations begin, it is possible to estimate the work function of the surface locally on an atomic scale. In addition, just as optical Fabry-Perot interferometers can be used for accurate measurement of distance scales, so can this electron interferometer be used to accurately calibrate the distance scale of the  $z$  motion of the microscope. In this way, we have obtained excellent agreement between measured and expected values of atomic step heights like those shown in Fig. 2.

The other region of electrical interest in the operation of the tunneling microscope is found roughly below 4 V of bias. Here tunneling proceeds through the entire vacuum gap region because the kinetic energy never becomes positive there. Nevertheless, structure in the curve of conductance versus bias may still be observed in this low-bias region. This structure is thought to be more characteristic of intrinsic variations of the density of allowed and accessible excited electron states at the surface into which tip electrons may tunnel (20). As distinct from the geometrical interference effects at high bias, we may expect that structure in the low-bias conductance curves may be more closely correlated with electronic consequences of microscopic atomic structure. For example, it might be hoped that certain kinds of impurity atoms will have distinct and easily identifiable features in these curves. Such hopes for simple interpretation of results in this region must be tempered by the fact that on atomically homogeneous surfaces complicated features may already be present due to the effects of local band structure. Figure 4 shows several peaks below 4 V of bias for the silicon surface discussed above. The detailed shape of the curves is different for data taken at two different positions on the surface separated by only 23 Å (curves b1 and b2 in Fig. 4). In the

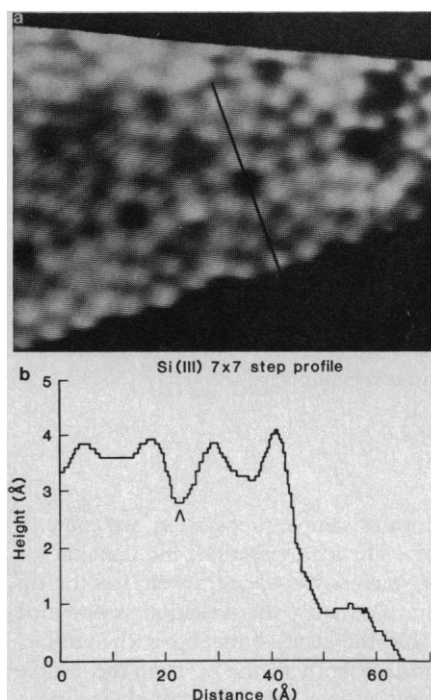


Fig. 6. (a) Tunneling image of silicon ( $7\times 7$ ) surface taken at a bias that enhances the asymmetry around the cell short diagonal. (b) Line scan showing the tip height along the dark line drawn normal to the step along a long diagonal. The asymmetry is clearly seen. The arrow at the dip in the scan line marks a cell corner depression.

preliminary topographical results (Figs. 2 and 3), these two positions, which were the midpoints of the two equilateral triangles that make up the  $7\times 7$  rhombic cell, appeared totally equivalent. Information like this must be correlated with other spectroscopic probes of the surface and calculations to unravel their significance (21). In this case, we have found that variations in the conduction band surface density of states can account for both the structure observed in Fig. 4 (curves 1b and 2b) and the differences between the curves if the latter is explained by a rearranged subsurface structure in part of the cell called a stacking fault.

At this stage, it is important to notice that, if different electronic features are observed for different gap biases, then one may anticipate that different structure may be visible in topographs taken at different biases. This effect is illustrated again for our silicon surface example. By applying the appropriate bias, an asymmetry across the short diagonal of the ( $7\times 7$ ) unit cell that was previously undetectable becomes clear (Fig. 6). We have associated this asymmetry with

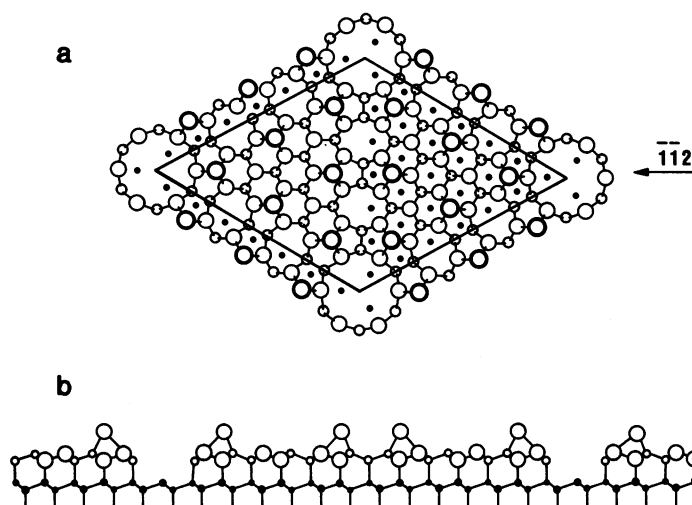


Fig. 7. Ball and stick model of the  $7\times 7$  surface reconstruction. Top and side views are shown with nearest atoms enlarged (22). The unit cell is drawn, within which the 12 top adatoms are seen as the largest balls.

subsurface structure associated with a model of the  $7 \times 7$  reconstruction (22). The point to emphasize here is that the simple view that tunneling images are maps of atomic density at a surface must be tempered by an awareness that the picture obtained is in general a mixture of spectroscopic and geometric information. Interpretation must therefore proceed with great caution, particularly for surfaces where little information from other surface probes is available.

One way around the problem of complex structurally related electronic effects in tunneling studies was introduced by Giaever (23), who showed that, when one side of the tunnel junction is a superconductor, the superconducting energy gap can be observed directly in conductance-type measurements. In addition, careful electrical characterization of low-temperature tunnel junctions has shown that by detecting the onset of inelastic tunneling channels (those associated with phonon excitation) the vibrational spectra of the surface regions of junction may be probed (24). Just as in the electronic case discussed above, the vibrational properties contain important clues to the constitution of the surface. Steps to extend these kinds of studies to the tunneling microscope have been taken at several laboratories, where liquid helium-cooled instruments have been built. In the most advanced work to date, C. Quate at Stanford University has demonstrated topographs whose contrast is controlled by the local superconducting gap parameters as well as by surface structure (25). The atomic scale observation of vibrational spectra with the tunneling microscope seems to be a difficult problem because of signal-to-noise limitations, but it may not be beyond the capabilities of the instrument.

## The Final Structure

Figure 7 shows what we believe to be the atomic structure of the silicon (111)  $7 \times 7$  unit cell. The top layer is the 12 adatoms so clearly seen in Figs. 2 and 3. The second layer, made visible only at special  $V_{\text{bias}}$  as in Fig. 6, consists of two triangular regions, one of which is a perfect termination of the lattice. The other is a stacking fault. This layer is rotated  $180^\circ$  around the surface normal to the unfaulted layer. These two triangular regions on each side of the cell short diagonal are "zipped" together by a structure consisting of five- and eight-sided rings, known to crystallographers as a  $60^\circ$  partial dislocation. This model was recently introduced to the surface physics community by Takayanagi *et al.* (22) to explain additional features of their high-energy electron microscopy results.

It accounts for the asymmetry across the short diagonal in the tunneling images with the triangular stacking fault. A simple model for the reconstruction of the atomic steps is also obtained (26).

It is difficult to conclude this brief survey of tunneling microscopy in any but an optimistic note. We can surely look forward to new insights on the geometric and the electronic properties of matter as well as progress on new instruments and methods to manipulate structures on an atomic scale. Solid-state physicists, material scientists, chemists, and biologists many well want to keep an eye on the tunneling microscope.

---

## REFERENCES AND NOTES

1. G. Binnig, H. Rohrer, C. Gerber, E. Weibel, *Phys. Rev. Lett.* **50**, 120 (1983).
2. E. W. Müller, *Z. Phys.* **131**, 136 (1951).
3. J. M. Cowley, *Diffraction Physics* (North-Holland, New York, 1984), chap. 13.
4. A. V. Crewe, J. Wall, J. Langmore, *Science* **168**, 1338 (1970); M. S. Isaacson, J. Langmore, N. W. Parker, D. Kopf, M. Utlaut, *Ultramicroscopy* **1**, 359 (1976).
5. K. Takayanagi, *Ultramicroscopy* **16**, 101 (1985).
6. R. Young, J. Ward, F. Scire, *Rev. Sci. Instrum.* **43**, 999 (1972).
7. G. Binnig, H. Rohrer, C. Gerber, E. Weibel, *Phys. Rev. Lett.* **49**, 57 (1982).
8. ———, *Surf. Sci.* **131**, L379 (1983).
9. W. P. Ellis and R. L. Schwoebel, *ibid.* **11**, 82 (1968); M. Henzler, *ibid.* **19**, 159 (1970).
10. H. C. Abbink, R. M. Broudy, G. P. McCarthy, *J. Appl. Phys.* **39**, 4673 (1968).
11. Y. Tanishiro, K. Takayanagi, K. Yagi, *Ultramicroscopy* **11**, 95 (1983).
12. R. S. Becker, J. A. Golovchenko, B. S. Swartzentruber, *Phys. Rev. Lett.* **54**, 2678 (1985).
13. R. Tromp, R. J. Hamers, J. E. Demuth, *ibid.* **55**, 1303 (1985).
14. R. M. Feenstra and G. S. Oehrlein, *Phys. Rev. B* **32**, 1394 (1985).
15. R. V. Coleman, B. Drake, P. K. Hansma, G. Slough, *Phys. Rev. Lett.* **55**, 394 (1985).
16. A. M. Baró *et al.*, *Nature (London)* **315**, 253 (1985).
17. R. Young, J. Ward, F. Scire, *Phys. Rev. Lett.* **27**, 922 (1971).
18. G. Binnig and H. Rohrer, *Helv. Acta* **15**, 726 (1982).
19. R. S. Becker, J. A. Golovchenko, B. S. Swartzentruber, *Phys. Rev. Lett.* **55**, 987 (1985).
20. J. Tersoff and D. R. Hamann, *ibid.* **50**, 1998 (1983); *Phys. Rev. B* **31**, 805 (1985); N. Garcia, C. Ocel, F. Flores, *Phys. Rev. Lett.* **50**, 2002 (1983); T. E. Feuchtwang, P. H. Cutler, N. H. Miskovsky, *Phys. Lett.* **99A**, 167 (1983); E. Stoll, A. Baratoff, A. Selloni, P. Carnevali, *J. Phys. C* **17**, 3073 (1984); N. D. Lang, *Phys. Rev. Lett.* **55**, 230 (1985).
21. R. S. Becker, J. A. Golovchenko, D. R. Hamann, B. S. Swartzentruber, *Phys. Rev. Lett.* **55**, 2032 (1985).
22. K. Takayanagi, Y. Tanishiro, M. Takahashi, S. Takahashi, *J. Vac. Sci. Technol.* **A3**, 1502 (1985).
23. I. Giaever, *Phys. Rev. Lett.* **5**, 147 (1960).
24. R. C. Jaklevic and J. Lamb, *ibid.* **17**, 1139 (1966); E. Burstein and S. Lundquist, Eds., *Tunneling Phenomena in Solids* (Plenum, New York, 1969), chap. 17.
25. A. L. de Lozanne, S. A. Elrod, C. F. Quate, *Phys. Rev. Lett.* **54**, 2433 (1985).
26. R. S. Becker, J. A. Golovchenko, E. G. McRae, B. S. Swartzentruber, *ibid.* **55**, 2028 (1985).
27. Many of the views and results reported here are the result of a fruitful collaboration over the years with my colleagues R. S. Becker and B. S. Swartzentruber. The constant support, advice, and encouragement of D. H. Auston and V. Narayana-murti are also deeply appreciated.